remote sensing

MDPI

Communication

Photometric Observations of Aerosol Optical Properties and Emission Flux Rates of Stromboli Volcano Plume during the PEACETIME Campaign

Pasquale Sellitto [1,*], Giuseppe Salerno [2], Jean-François Doussin [1], Sylvain Triquet [3], François Dulac [4] and Karine Desboeufs [3]

1 Univ. Paris Est Créteil and Université de Paris, CNRS, Laboratoire Interuniversitaire des Systèmes Atmosphériques, Institut Pierre Simon Laplace, F-94010 Créteil, France; doussin@lisa.ipsl.fr
2 Istituto Nazionale di Geofisica e Vulcanologia, Osservatorio Etneo, I-95125 Catania, Italy; giuseppe.salerno@ingv.it
3 Université de Paris and Univ Paris Est Creteil, CNRS, LISA, IPSL, F-75013 Paris, France; sylvain.triquet@lisa.ipsl.fr (S.T.); karine.desboeufs@lisa.ipsl.fr (K.D.)
4 Laboratoire des Sciences du Climat et de l'Environnement (LSCE), UMR 8212 CEA-CNRS-UVSQ, Institut Pierre-Simon Laplace, Univ. Paris-Saclay, F-91191 Gif-sur-Yvette, France; francois.dulac@lsce.ipsl.fr
* Correspondence: pasquale.sellitto@lisa.ipsl.fr

Abstract: The characterisation of aerosol emissions from volcanoes is a crucial step towards the assessment of their importance for regional air quality and regional-to-global climate. In this paper we present, for the first time, the characterisation of aerosol emissions of the Stromboli volcano, in terms of their optical properties and emission flux rates, carried out during the PEACETIME oceanographic campaign. Using sun-photometric observations realised during a near-ideal full plume crossing, a plume-isolated aerosol optical depth of 0.07–0.08 in the shorter-wavelength visible range, decreasing to about 0.02 in the near infrared range, was found. An Ångström exponent of 1.40 ± 0.40 was also derived. This value may suggest the dominant presence of sulphate aerosols with a minor presence of ash. During the crossing, two separate plume sections were identified, one possibly slightly affected by ash coming from a mild explosion, and the other more likely composed of pure sulphate aerosols. Exploiting the full crossing scan of the plume, an aerosol emission flux rate of 9–13 kg/s was estimated. This value was 50% larger than for typical passively degassing volcanoes, thus pointing to the importance of mild explosions for aerosol emissions in the atmosphere.

Keywords: volcanic plumes; volcanic aerosols; Stromboli volcano; sun-photometry; aerosol optical properties; aerosol emission rate

Citation: Sellitto, P.; Salerno, G.; Doussin, J.-F.; Triquet, S.; Dulac, F.; Desboeufs, K. Photometric Observations of Aerosol Optical Properties and Emission Flux Rates of Stromboli Volcano Plume during the PEACETIME Campaign. *Remote Sens.* **2021**, *13*, 4016. https://doi.org/10.3390/rs13194016

Academic Editor: Andrew McGonigle

Received: 30 July 2021
Accepted: 1 October 2021
Published: 8 October 2021

1. Introduction

Through their varied and diverse activity, volcanoes emit both gaseous and particulate species that can affect the downwind atmospheric composition [1,2], aerosol layer [2,3], radiative balance [4,5] and cloud occurrence [6,7] at different spatiotemporal scales and in both the troposphere and the stratosphere. In particular, volcanic emissions are an important source of aerosol particles for the Earth's atmosphere. Depending on their internal geochemical and geophysical processes, volcanoes can emit two types of aerosol: primary mineral ash and primary (see case-study in [8]) or secondary sulphate aerosol (SA). Ash is mainly produced by magma solidification when, after fragmentation due to eruptive processes, it enters in contact with the atmosphere. Secondary sulphate aerosols are formed by gas-to-particle conversion of primary sulphur dioxide (SO_2) gaseous emissions, during both explosive and quiescent degassing. Past analyses suggest that 14% to 36% of the global tropospheric SA burden may be volcanogenic [9,10]. Recent studies have highlighted that SA is also present in the young near-source plumes emanating from volcanoes that degas, more or less continuously, to the atmosphere, e.g., [4,11,12]. On the opposite end of the spectrum of volcanic activity types,

explosive eruptions are well known to impact the upper-tropospheric—lower-stratospheric aerosol budget and properties, with higher-altitudes injections of both fine ash and secondary SA [13].

The characterisation of aerosol emissions from volcanoes and their atmospheric dispersion and aging processes, using remote-sensing techniques, is a powerful tool to link these emissions with their downwind impacts on the air quality and the radiative balance. Satellite-borne, e.g., [14], air-borne, e.g., [15] and ground-based, e.g., [16,17] techniques have all been proposed, in the past, to characterise volcanic aerosols at relevant spatiotemporal scales, as well as their synergies [18,19]. These observations and their synergies allowed the estimation of the impacts of volcanic emission on the climate system from the local [4] to the regional [18,20] to the global scale [21].

The near-crater characterisation of aerosol emissions is one important step towards larger-scale estimations of the impacts of volcanic emission. This is particularly important for continuously degassing volcanoes. One notable example of a continuously degassing volcano is Stromboli, Italy. In the present paper we present the characterisation of aerosol emissions of the Stromboli volcano in the western Mediterranean, in terms of their optical properties and emission flux rates, carried out during the PEACETIME oceanographic campaign [22]. Very few past works dealt with the characterisation of aerosol properties from the Stromboli volcano [23–25]. To the best of our knowledge, this is the first estimation of Stromboli aerosol emissions and optical properties using remote-sensing techniques and the first estimation overall of Stromboli aerosol emission rates.

The present manuscript is structured as follows. In Section 2, the geological framework of Stromboli volcano, its activity style and its conditions during the measurement campaign are introduced. In Section 3, the observation methodologies are discussed. Results are presented and discussed in Section 4. Finally, conclusions are drawn in Section 5.

2. Stromboli Volcano and Its Activity during the Measurement Campaign

Stromboli is the emergent portion of a ~3.4 km high stratovolcano rising up to about 920 m above sea level from the Tyrrhenian Sea off South Italy, (38°48′N, 15°13′E; Figure 1a,b). The volcano, world-known for its mild and uninterrupted Strombolian activity [26], is famous for its eruptive style, that has become the archetype of "Strombolian activity": intermittent, mild explosions (Figure 1a) of incandescent lava fragments (bombs and lapilli) ejected up to 100–200 m height above the crater terrace occurring on average every 5–20 min e.g., [26–28]. The explosive activity of Stromboli is also characterized by occasional more violent than ordinary explosive events named based on their intensity in major explosions and paroxysms, e.g., [27,29]. Stromboli also generates effusive eruptions of magma from fissures typically opening on the upper flanks and supplying lava flows confined within the Sciara del Fuoco slope, e.g., [30–32]. The persistent eruptive activity of Stromboli is fed by a volatile-rich high-potassium arc basalt whose continuous degassing through open conduits sustains a permanent volcanic plume degassing, which contribute 1–2% of the estimated global volcanic yield of sulphur, halogens, and trace metals to the atmosphere [33]. Considering an average explosion frequency of six per hour and duration $\leq$10 s each, the active syn-explosive degassing represents only about 2% of the emissions; therefore, the quiescent gas venting accounts for about 98% of the volcanic activity, thus contributing to largely most of the gas output of Stromboli [34]. Chemical investigation of Stromboli's plume degassing has revealed a large spread of plume compositions depending on bulk-quiescent and sin-explosive degassing. The quiescent degassing shows a well-defined time-averaged chemical composition dominated by H_2O (48–98 mol%; mean 80%), CO_2 (2–50 mol%; mean 17%) and SO_2 (0.2–14 mol%; mean 3%), e.g., [35]. SO_2 represents by far the main sulphur species: SO_2/H_2S molar ratios range from 14 to 17 [36] and particulate sulphur accounts for $\leq$5% of total sulphur [33]. Compared with quiescent emissions, the bursting gas slugs associated with the ordinary Strombolian explosive activity have a distinct chemical composition. The gas phase is richer in CO_2 (11–50%; mean 26%) and poorer in H_2O (48–88%; mean, 73%) than the bulk plume passively released by the volcano, and moreover display higher CO_2/SO_2, SO_2/HCl, and CO/CO_2 molar ratios, e.g., [35,37]. Among trace elements, Stromboli's plume

contains a proportion of bromine and highly volatile metalloids and metals with sulphur affinity (such as Se, Cd, Bi, In, and As) are the most enriched [33]. The contribution of aerosol particles produced by condensation of the magmatic gas phase in the atmosphere was estimated to be 66% of the total aerosol volume [33], with a rapid growth near the vents but also occurring efficiently along the plume dispersion at distances farther than 35 km [24]. Near-source soluble sulphate particles were observed rich in SO_4^{2-}, H^+, Na^+, K^+ and NH_4^+ ions, with concentration ranging between 0.94–2.14 μmol m^{-3} and aerosol size distribution essentially monomodal. Condensation nuclei have been observed in Stromboli plume, with maximum concentration localized close to the vent [25]. Based on in situ optical and morphological measurements, the aerosol particles of Stromboli degassing plumes result to be porous with 18–35% of air voids in terms of the total volume [26].

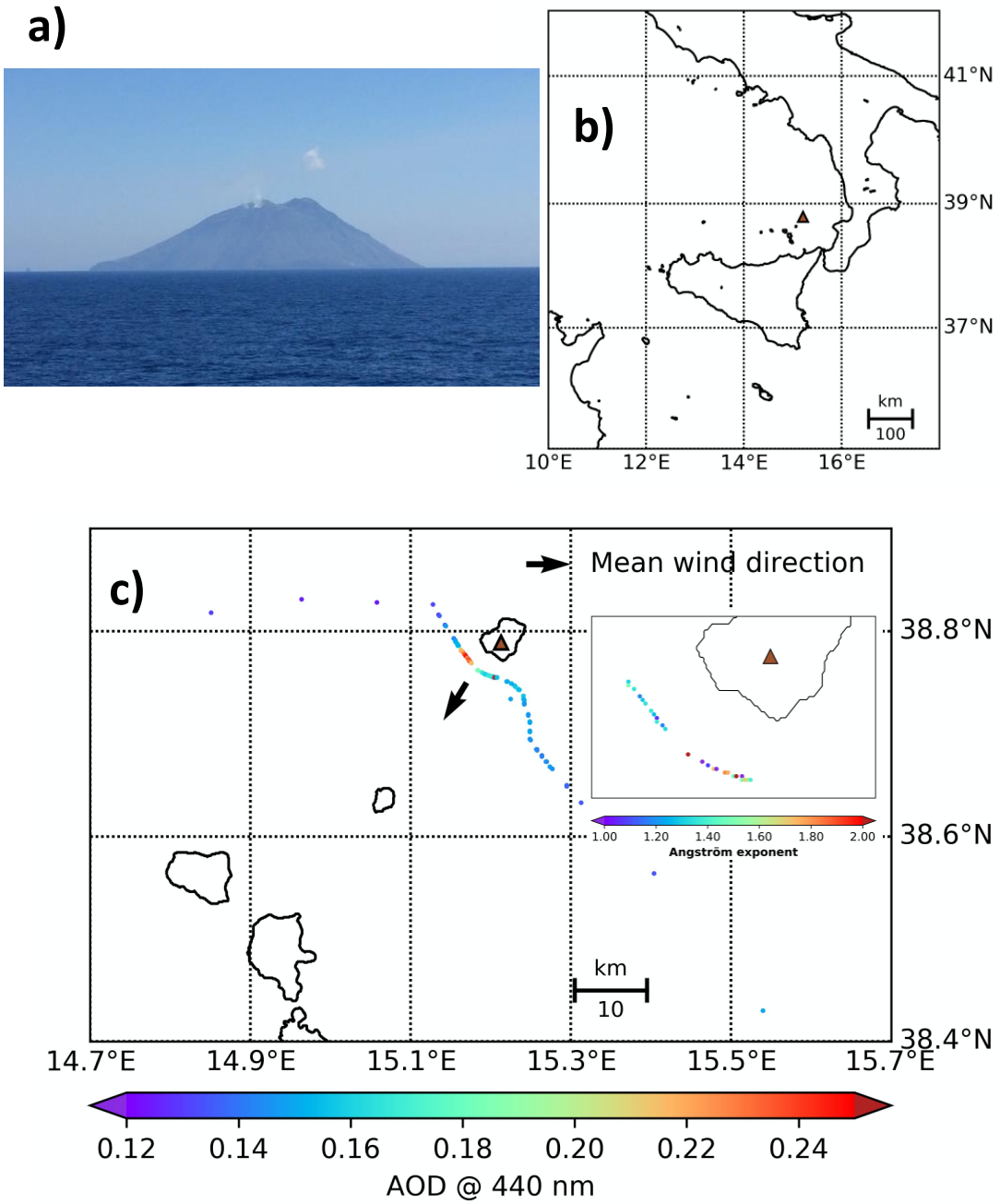

Figure 1. (**a**) Picture of Stromboli volcano during the measurement campaign, with a typical Strombolian explosion visible. (**b**) Location of Stromboli volcano (brown triangle) in the wider context of southern Italy. (**c**) MicroTops-II (MII) sun-photometric AOD observations at 440 nm before, during and after the section scan on Stromboli plume. The black arrow

shows the average wind direction during the plume crossing. The Ångström exponent (440/675 nm) for the section scan is shown in the inlet of panel c.

During the day of our survey, the volcanic aerosol measurements and features of which are reported here (22 May 2017), the volcano showed its typical activity, with rhythmic Strombolian explosions of variable energy, from different vents, at an average frequency of 15–20 events per hour (see open-file reports at www.ct.ingv.it and ref. [38]). The daily average SO_2 flux observed remotely by means of the FLAME (FLux Automatic MEasurements) scanning DOAS (differential optical absorption spectroscopy) network was of ~230 10^3 kg d^{-1}.

3. Data and Methods

3.1. The PEACETIME Campaign

The PEACETIME oceanographic campaign (https://doi.org/10.17600/17000300) took place in the western and central Mediterranean between 11 May and 10 June 2017 on board the French research vessel "Pourquoi Pas?". The main target of the PEACETIME campaign was to better understand air-sea interface processes after atmospheric deposition in the Mediterranean Sea. Shipboard determinations of marine and atmospheric parameters were made from atmospheric and ocean underway, as well from water-column sampling stations that were occupied during the cruise [22]. During the cruise, on 22 May 2017, the vessel passed close-by the Stromboli volcano and a short dedicated measurement session, while crossing the volcanic plume, was realised. The "Pourquoi Pas ?" vessel had the PEGASUS platform onboard, which is a collection of atmospheric in situ instruments; none of them reveals any sign of volcanic influence on the surface air composition. This absence of increase in particulate matter concentration, SO_2 concentration or sulphate occurrence indicates that the Stromboli plume, emitted at an altitude higher than 900 m, was likely confined in the free troposphere. Indeed, the LiDAR measurements on board the vessel (unfortunately not working on the day of the crossing) have detected a marine boundary layer heights lower than 500 m during most of the cruise, as it is expected over the Mediterranean Sea under these weather conditions [39]. Our detection of the Stromboli plume relied mostly on sun-photometric observations which are described in Section 3.2 and are discussed in the present paper.

3.2. Observations of Volcanic Aerosols' Optical Properties with a MicroTops Sun-Photometer

Aerosol optical properties of the Stromboli plume were derived on 22 May 2017, during the PEACETIME campaign, using a hand-held MicroTops-II (MII) sun-photometer [40]. The MII instrument is very light (about 600 g), thus allowing agile observations based on movable platforms like ships [41]. The MII instrument measures direct sun radiance at relatively small field of view (2.5°). The specific model used during this campaign (s/n 17879) has four channels in the atmospheric-window visible spectral range (Ch.1: 380.0 ± 0.4 nm, with nominal FWHM of 4.0 nm, and Ch.2: 440.0 ± 1.5, Ch.3: 500.0 ± 1.5 and Ch.4: 675.0 ± 1.5 nm, with nominal FWHM of 10.0 nm), as well as one channel in the near infrared spectral range (Ch.5: 1020.0 ± 1.5 nm, with nominal FWHM of 10.0 nm), used to derive the aerosol optical depth (AOD) at these wavelengths. The manual sun-pointing is performed with the aid of a sun target window which displays an optical projection of the sun-disk position with respect to the input optics section of the instrument. The instrument used during the campaign was Langley pre-calibrated at the Service d'Observation PHOTONS in April 2017. The AOD uncertainties are typically dominated by: 1) calibration uncertainties, 2) measured signal error, which is mostly dependent on pointing errors and electronic noise, 3) errors linked to Rayleigh scattering and gaseous absorption corrections (e.g., ozone absorption correction for Ch.1). While all these error sources are limited, e.g. [40,41], pointing errors during ship-based observations require special care to avoid larger error contributions. As discussed by Porter et al. [41], we limited pointing-errors by using short time acquisitions and by excluding aberrant larger AOD

values from the dataset. Taking care of pointing errors, the theoretical uncertainties of our MII AOD can be estimated <±0.02 [41].

The AOD at the five wavelengths, from Ch.1 to Ch.5, of vertically confined and geometrically thin plumes, like for volcanic plumes, are obtained by atmospheric background correction as described in detail by, for example, Sellitto et al. [16]. When the direct sun observation is performed as to traverse a confined aerosol plume, the measured AOD (AOD_T) is the addition of the plume (AOD_P) and atmospheric background (AOD_B) AODs:

$$AOD_T(\lambda) = AOD_P(\lambda) + AOD_B(\lambda) \quad (1)$$

then, the AOD_P can be isolated by subtracting an estimation of AOD_B from the in-plume AOD_T observations. The atmospheric background AOD_B can be estimated with the acquisition of MII AOD observations in regions free of the confined plume aerosols but not spatiotemporally too far from the in-plume acquisitions, in order to ensure that the atmosphere remains reasonably homogeneous between background and in-plume observations. It is also assumed that the clear atmosphere aerosol optical depth in the volume occupied by the plume is negligible with respect to the overall columnar AOD_B. With the aforementioned atmospheric background correction, it is then possible to obtain five-wavelengths spectra of the volcanic plume $AOD_P(\lambda)$.

The AOD variation with wavelength λ can be modelled using the empirical Ångström law:

$$AOD_P(\lambda) = \beta\lambda^{-AE} \quad (2)$$

where β is the AOD at a reference wavelength (λ = 1000 nm) and AE is the so called Ångström exponent of the confined plume. The AE is an optical proxy of the mean size of the aerosol layer, that has been used in past observations of volcanic plumes as an empirical discriminant parameter to distinguish between larger ash particles and smaller SA [e.g., 4, 42]. Thus, the plume's AE can be derived using the AOD_P at two wavelengths, as follows:

$$AE = -\frac{ln\frac{AOD(\lambda_1)}{AOD(\lambda_2)}}{ln\frac{\lambda_1}{\lambda_2}} \quad (3)$$

the volcanic plume's AE observations discussed in this paper are derived using the AOD_P for channels at 440.0 (Ch.2) and 675 nm (Ch.4). The AE is a bulk optical proxy for particle mean size in an aerosol plume. Bigger AEs are generally linked to smaller particles, on average, in the sampled plume and vice versa. The plume's AE values larger than e.g., 1.0–1.5 have been associated to volcanic SA and smaller values to the possible presence of ash, e.g., [4,42]. Based on the discussion of Sellitto et al. [4], the theoretical uncertainties of the atmospheric-window AE derived by MII is expected to be <±0.2 (<±15%), for typical conditions during the campaigns.

3.3. Estimation of the Aerosol Mass Flux

As discussed by Porter at al. [17], starting from a complete transversal section crossing scan of a horizontally confined aerosol plume, based on a series of AOD measurements of the plume, the aerosol mass flux rate AFR can be calculated as:

$$AFR = \frac{w_s}{MEC}\sum_i D_i * AOD_i \quad (4)$$

where MEC is the mass extinction coefficient of the aerosol layer, AOD_i is the plume's aerosol optical depth measurement, at the same wavelength of MEC, for the section interval i of width D_i and w_s is the average wind speed (providing that the wind speed and direction is relatively constant during the crossing scan). As we have identified two different sections of the plume, with different optical properties (see Table 1), we calculate mass flux for them separately:

$$AFR_1 = \frac{w_s}{MEC_1} \sum_{i=\{j\}} D_i * AOD_i \quad (5)$$

$$AFR_2 = \frac{w_s}{MEC_2} \sum_{i=\{k\}} D_i * AOD_i \quad (6)$$

In Equations (5) and (6), the indices 1 and 2 refer to plume sections 1 and 2 and *j* and *k* refer to corresponding section intervals in the overall plume section discretisation (the indices i in Equation (4)).

4. Results and Discussion

4.1. Optical Characterisation of the Stromboli Plume

Figure 1c shows the MII sun-photometric AOD_T observations at 440 nm during the approach, the cross-scan and after the crossing of the volcanic plume emitted from Stromboli volcano, during the PEACETIME campaign. Complementary radiation measurements, with an on-board sky radiometer, show that the sky was cloud free during this time interval. As is clearly visible from the figure, a different typical cluster of AOD values can be found that can empirically be associated to the atmospheric background and separate sections of the plume: 1) moderate AOD values further from the volcano, both at the beginning and at the end of the measurement session, 2) a first marked increase of the AOD_T closer to the volcano, 3) a second cluster of enhanced AOD_T, larger than those of point 1 but smaller than those of point 2. The AOD_T observations of point 1 can easily be attributed to the atmospheric background. During this cluster of observations, at larger distance from the volcano, we were not under the plume. The AOD_T observations of point 2 and 3 can be attributed to the Stromboli plume, as confirmed by visual observations during the crossing (Figure 1a), and are further discussed in the following section.

Based on this first discrimination, we then carried out the atmospheric background correction of Equation (1) and isolated the AOD_P values for the Stromboli plume. Figure 2 shows the average AOD spectral values at the five MII channels for the atmospheric background $AOD_B(\lambda)$ (average of section 1) and the isolated Stromboli plume $AOD_P(\lambda)$ (average of atmospheric-corrected sections 2 and 3). The atmospheric background AOD_B has typical values of about 0.14–0.18 in the shorter-wavelength visible range, decreasing to about 0.04 in the near infrared range. Background AOD values of about 0.12–0.15, in the visible spectral range, are also observed by Aqua-MODIS (MODerate resolution Imaging Spectrometer) satellite instrument in the area, a few hours later our campaign (not shown here), thus confirming our MII background AOD. We found moderate AOD_P values for the Stromboli plume, with typical values of about 0.07–0.08 in the shorter-wavelength visible range, decreasing to about 0.02 in the near infrared range. At this very proximal location from the emitting crater (less than 5 km), the Stromboli plume had, during this campaign, slightly smaller AOD_P values than past AOD_P observations of near-crater plumes of nearby Mount Etna volcano in passive degassing conditions (around 0.1 in the visible spectral range) and significantly smaller values than in the case of mild explosive activity of Mount Etna (in some cases exceeding 0.2 in the visible spectral range) [4,16]. Figure 2 also shows the variability of the AOD_B and AOD_P in terms of the standard deviation of their spectral mean values. It is apparent how the background-identified AODs have a significantly smaller variability, if compared with volcanic-plume's AODs. This corroborates our identification of the background and plume sections of the measurement session: proximal naturally-emitted plumes, like from volcanic activity [16,20] or fire emissions [43], are expected to be more inhomogeneous in terms of composition, density and particle size distribution than the atmospheric background aerosol layer or for plumes dispersed at larger spatiotemporal scales.

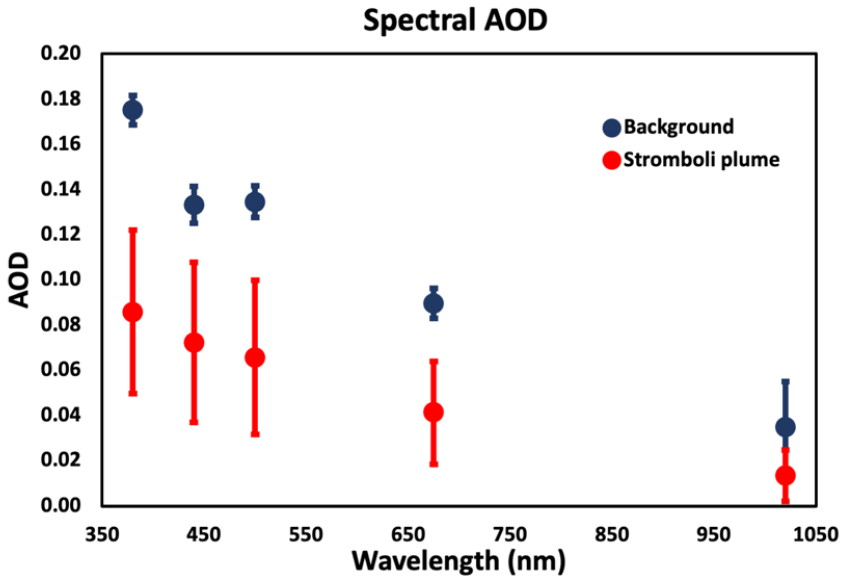

Figure 2. Average spectral AOD observations of the atmospheric background (in blue, $AOD_B(\lambda)$) and of the isolated Stromboli plume (in red, $AOD_P(\lambda)$), after the atmospheric background correction of Equation (1). The error bars of the spectral AODs represents the standard deviation of their means, linked to the AODs variability.

Using the information coming from the spectral variability of its AOD_P spectra, summarised by the AE of the Stromboli plume, below we analyse this isolated volcanic plume in more detail. The spatial distribution of the central part of the plume's AE, closer to the volcano, is shown in the inlet of Figures 1c and 3 shows the time series of the AOD_P observations during the measurement session, at three selected wavelengths (380, 440 and 675 nm). The plume's AE, calculated using Equation (3), is also shown in Figure 3. As introduced above, two separate cluster of AOD_P and AE are found in the plume: a first cluster with larger AOD_P and smaller AE and a second cluster with smaller AOD_P and larger AE. The mean and extreme values for these two sections (hereafter referred to as plume's Sections 1 and 2) are summarised in Table 1 and compared with the overall plume's and the background averages. Section 1 has an average AOD_P value of 0.10 ± 0.01 at 440 nm and an average AE value of 1.23 ± 0.25, with AE values not exceeding 1.5. Section 2 has an average AOD_P value of 0.05 ± 0.03 at 440 nm and an average AE value of 1.57 ± 0.46, with AE values exceeding the very high value of 2.3. Section 2 has AODP/AE combination values which are typical of passive degassing plumes [42]. In general, small values of the AOD_P and AE exceeding 1.5 have been associated with ash-free volcanic plumes, dominated by tiny secondary SA particles. This looks like the case for Section 2. While plume's Section 1 has not the typical extremely small AE values of ash-bearing plumes (smaller than 1.0 and down to 0.0 in some extreme cases [42]), the values found here seem to suggest the possible presence of at least a small fraction of fine ash, even if the presence of larger water droplets, due to sustained water vapour condensation, cannot be excluded. Seismic data at the Stromboli volcano (not shown here) for this specific case, display a short-lasting peak in the amplitude of the seismogram traces that is very likely linked to a mild explosion at about 11:15 UTC, followed by a flat seismic signal afterwards. This supports the hypothesis that the two identified plumes sections can be associated to an explosive event (Section 1) and passive degassing (Section 2). We then conclude that Sections 1 and 2 definitely have different characteristics, in terms of the aerosol burden and size distribution, with possible ash in Section 1, due to a mild explosion, and ash-free conditions in Section 2, associated to the absence of explosions. A clear spatial separation of these two plumes' sections, with smaller AE in the first part of the plume crossing and larger AE afterwards, can be seen in Figure 1c.

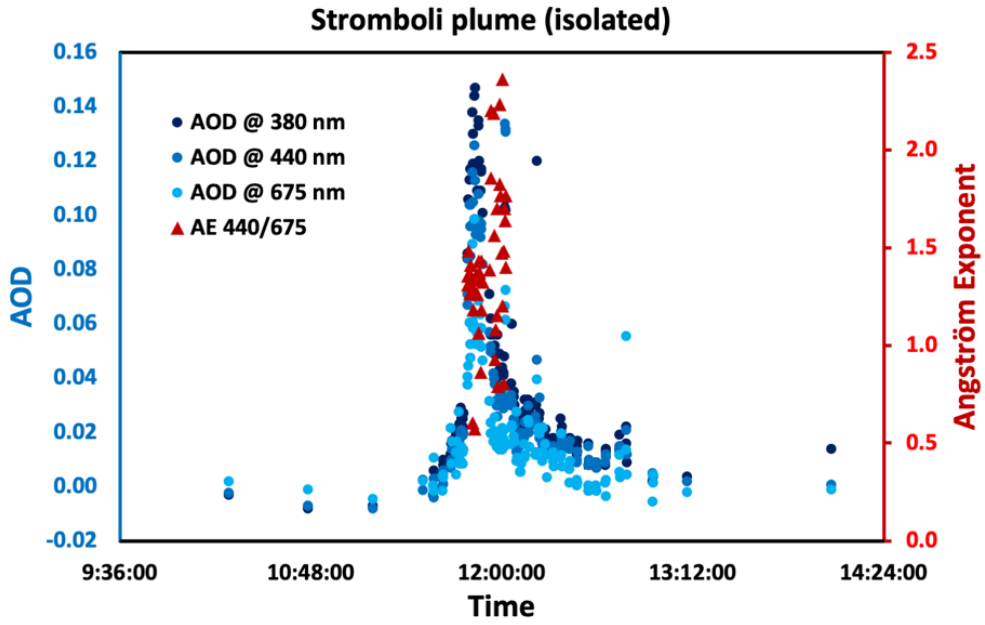

Figure 3. Atmospheric background corrected plume-isolated AOD_P for Stromboli plume at 380 (dark blue dots), 440 (blue dots) and 675 nm (sky blue dots), and plume's AE (red triangles). Time is UTC.

Table 1. Average AE and AOD_P at 440 nm for the two identified plume's Sections 1 and 2 (see text for details). The averages are displayed with their standard deviation, and maximum/minimum values interval. As a comparison, also the whole plume and atmospheric background values are reported.

Plume Section	AE	AOD_P (440 nm)
Section 1	1.23 ± 0.25; 0.57/1.48	0.10 ± 0.01; 0.07/0.13
Section 2	1.57 ± 0.46; 0.79/2.36	0.05 ± 0.03; 0.03/0.13
Whole plume	1.40 ± 0.40	0.08 ± 0.04
Background	0.93 ± 0.12	0.13 ± 0.01

As this is the first time spectral AODs for the Stromboli plume are reported, more observations are required to characterise the likely spatiotemporal variability of both AOD_P and AE values for this volcano.

4.2. Aerosol Mass Flux Rate

We provide here a raw estimation of the aerosol mass emission flux rate, using the method summarised by Equations (5) and (6).

For the two plume clusters identified in Section 4.1, the same wind speed w_s has been used. The wind speed, measured locally at Stromboli observatory, stayed relatively constant in both intensity and direction, during the plume crossing. Based on this dataset, a wind speed of 1.73 m/s with the direction as indicated in Figure 1c is used. It can be noted how the plume crossing was realised in optimal conditions, i.e., with a quasi-perpendicular plume crossing. Limited errors can arise from the local non-perpendicularity of the scan. Due to the different AOD spectral variability, pointing at a different aerosol size distribution and, possibly, at a limited presence of ash in plume Section 1, the mass extinction coefficients MEC in the two plume sections have been considered different. We used a typical MEC interval for pure sulphate aerosols for Section 2, a minimum of 8 $m^2\ g^{-1}$ and a maximum of 10 $m^2\ g^{-1}$, which are reference MEC values in the visible spectral range, around 500 nm, for SA particles [44]. Note that these reference MEC values are global average of this parameter, for SA particles, which is most likely associated to aged SA. In this case, SA are freshly nucleated and the MEC value can differ from aged SA, thus introducing further uncertainty in AFR estimations. For Section 1, we hypothesised the presence of a small amount of ash,

possibly arising from the previous Strombolian explosion detected by the seismic signature mentioned in Section 4.1. Typical MEC for ash, around 500 nm, range between 2 and 3 m^2 g^{-1} [45]. As the AE observations for Section 1 do not point to a largely dominant ash component, we have empirically selected a MEC, for this cluster, ranging from 6 m^2 g^{-1} and a maximum of 8 m^2 g^{-1}. It is important to stress that this choice is somewhat arbitrary, so our estimations of the aerosol flux rate AFR1 for Section 1 must be taken with extreme caution. Using these constraints and hypotheses, we obtain an AFR1 of 5 to 7 kg s^{-1} and an AFR2 of 4 to 6 kg s^{-1}. The total AFR for Stromboli, during this measurement session, is then in the range 9–13 kg s^{-1}. Even if the two plume sections are characterised by roughly the same linear path length, the ashy Section 1 of the plume brings a slightly larger particles emission flux rate than the pure SA Section 2. In fact, the combination of smaller MEC and larger AOD associated to an ashy plume has the consequence that AFR_1 is larger than AFR_2. Mild explosions can have an important role as supply of aerosols to the atmosphere. These values of the AFR for Stromboli can be compared to the AFR observed at the nearby Mount Etna volcano. Watson and Oppenheimer [46] estimated the AFR at Mount Etna, using a similar method as that described in the present work and with MII observations, during a passive degassing activity phase, and found between 4.5 and 8.0 kgs^{-1}. Thus, even if comparable, our estimations for Stromboli are slightly larger than for a typical passively degassing activity, pointing to the larger impact on particle emissions of a mildly explosive Strombolian activity.

5. Conclusions

The characterisation of aerosol emissions from volcanoes is a very important step towards the estimation of their impact on the aerosol layer properties downwind, the regional air quality and the regional- to larger-scale radiative balance and climate. This is particularly important for continuously degassing volcanoes like Stromboli. In this paper, we have presented the first characterisation of the Stromboli aerosol plume, using a MII sun-photometer. A quasi-ideal full scan perpendicular crossing of the Stromboli plume was realised during the PEACETIME oceanographic campaign, on 22 May 2017. Using an atmospheric background correction, the AOD of the plume, at five wavelengths in the visible and near-infrared spectral region, was isolated. Average AOD values of 0.07–0.08 in the shorter-wavelength visible range, around 400 nm, decreasing to about 0.02 in the near infrared range, were found. This points to a relatively thin plume, if compared to the atmospheric background (0.14–0.18 in the shorter-wavelength visible range, to about 0.04 in the near infrared range). Using the AOD spectral variability provided by the MII sun-photometer, the AE of the plume could also be derived. The average AE for the plume was estimated at 1.40 ± 0.40, thus indicating the possible dominant presence of very small particles like sulphate aerosols, or in any case small particles, with a minor presence of the larger ash particles. During the crossing, two separate plume sections were identified. A first cluster of observations, during the crossing, was characterised by significantly larger AODs and smaller AE, thus pointing to the possible presence of ash coming from a mild explosion, that were visible during the approach of the vessel towards the plume and is confirmed by seismological data. A second cluster of observations was characterised by significantly smaller AODs and larger AE, thus indicating that this plume section is more likely composed of pure sulphate aerosols or, in any case, without ash—seismological data do not show further explosions, thus corroborating this hypothesis. The near textbook example of the crossing (i.e., quasi-perpendicular to the wind direction and then the plume dispersion orientation) allowed a raw estimation of the AFR for the Stromboli plume. An aerosol emission flux rate of 9–13 kg/s was estimated. This value is comparable to AFRs observed for the nearby Mount Etna volcano during passive degassing activity, but about 50% larger. This points to the importance of mild explosions for the supply of aerosol to the atmosphere. More studies are needed to better determine the aerosol optical properties and emission fluxes of Stromboli volcano, as well as their impact on the radiation balance.

Author Contributions: Data acquisition, J.-F.D. and K.D; Measurement conceptualisation, F.D., S.T. and K.D.; Data Analysis and Methodology, P.S.; Formal Analysis, P.S.; Investigation and Data Interpretation, P.S. and G.S.; writing—original draft preparation, P.S., G.S. and K.D. Writing—review and editing, all authors; Supervision of the PEACETIME campaign, K.D. All authors have read and agreed to the published version of the manuscript.

Funding: The "Pourquoi Pas?" campaign has been funded by CNRS-INSU, IFREMER, CEA and Météo-France.

Data Availability Statement: The MII datasets used in this work are available via the online AERONET/MAN QA/QC controlled dataset at the following link: https://aeronet.gsfc.nasa.gov/new_web/cruises_new/PourquoiPas_17.html (accessed on 6 October 2021).

Acknowledgments: We wish to thank, Thierry Alix, the captain of the R/V "Pourquoi Pas?" as well as the whole crew for its indefatigable involvement in our scientific activities. This study is a contribution to the PEACETIME project (http://peacetime-project.org; last access 4 May 2021), a joint initiative of the MERMEX and ChArMEx components supported by CNRS-INSU, IFREMER, CEA and Météo-France as part of the decadal programme MISTRALS coordinated by CNRS-INSU. The PHOTONS service (http://www-loa.univ-lille1.fr/photons) and in particular Thierry Podvin, Luc Blarel and Gaël Dubois are gratefully acknowledged for the maintenance and pre- and post-campaign calibrations of the MII sun-photometer used in this study. On board data that were used in this paper to verify that the Stromboli plume was confined above the boundary layer were obtained using the French PEGASUS mobile platform, a shared facility of the LISA/EFLUVE institutes (www.pegasus.cnrs.fr (accessed on 6 October 2021). The seismological data used in this work to verify possible mild volcanic explosions during the measurement session are courtesy of Ornella Cocina of INGV.

Conflicts of Interest: The authors declare no conflict of interest.

References

1. Von Glasow, R.; Bobrowski, N.; Kern, C. The effects of volcanic eruptions on atmospheric chemistry. *Chem. Geol.* **2009**, *263*, 131–142. [CrossRef]
2. Sellitto, P.; Zanetel, C.; di Sarra, A.; Salerno, G.; Tapparo, A.; Meloni, D.; Pace, G.; Caltabiano, T.; Briole, P.; Legras, B. The impact of Mount Etna sulfur emissions on the atmospheric composition and aerosol properties in the central Mediterranean: A statistical analysis over the period 2000–2013 based on observations and Lagrangian modelling. *Atmos. Environ.* **2017**, *148*, 77–88. [CrossRef]
3. Kremser, S.; Thomason, L.; von Hobe, M.; Hermann, M.; Deshler, T.; Timmreck, C.; Toohey, M.; Stenke, A.; Schwarz, J.P.; Weigel, R.; et al. Stratospheric aerosol-observations, processes, and impact on climate. *Rev. Geophys.* **2016**, *54*, 278–335. [CrossRef]
4. Sellitto, P.; Salerno, G.; La Spina, A.; Caltabiano, T.; Scollo, S.; Boselli, A.; Leto, G.; Zanmar Sanchez, R.; Crumeyrolle, S.; Hanoune, B.; et al. Small-scale volcanic aerosols variability, processes and direct radiative impact at Mount Etna during the EPL-RADIO campaigns. *Sci. Rep.* **2020**, *10*, 15224. [CrossRef] [PubMed]
5. Robock, A.; Oppenheimer, C. *Volcanism and the Earth's Atmosphere, Geophysical Monograph*; AGU: Washington, DC, USA, 2003; Volume 139.
6. Ebmeier, S.K.; Sayer, A.M.; Grainger, R.G.; Mather, T.A.; Carboni, E. Systematic satellite observations of the impact of aerosols from passive volcanic degassing on local cloud properties. *Atmos. Chem. Phys. Discuss.* **2014**, *14*, 10601–10618. [CrossRef]
7. Campbell, J.R.; Welton, E.J.; Krotkov, N.A.; Yang, K.; Stewart, S.A.; Fromm, M.D. Likely seeding of cirrus clouds by stratospheric Kasatochi volcanic aerosol particles near a mid-latitude tropopause fold. *Atmos. Environ.* **2012**, *46*, 441–448. [CrossRef]
8. Sellitto, P.; Guermazi, H.; Carboni, E.; Siddans, R.; Burton, M. Unified quantitative observation of coexisting volcanic sulfur dioxide and sulfate aerosols using ground-based Fourier transform infrared spectroscopy. *Atmos. Meas. Tech.* **2019**, *12*, 5381–5389. [CrossRef]
9. Graf, H.-F.; Feichter, J.; Langmann, B. Volcanic sulfur emissions: Estimates of source strength and its contribution to the global sulfate distribution. *J. Geophys. Res.* **1997**, *102*, 10727–10738. [CrossRef]
10. Stevenson, D.; Johnson, C.E.; Collins, W.; Derwent, R. The tropospheric sulphur cycle and the role of volcanic SO_2. *Geol. Soc. Spec. Publ.* **2003**, *213*, 295–305. [CrossRef]
11. Allen, A.G.; Oppenheimer, C.; Ferm, M.; Baxter, P.J.; Horrocks, L.A.; Galle, B.; Mcgonigle, A.J.S.; Duffell, H.J. Primary sulfate aerosol and associated emissions from Masaya Volcano, Nicaragua. *J. Geophys. Res.* **2002**, *107*, 4682. [CrossRef]
12. Mather, T.A.; Tsanev, V.I.; Pyle, D.; Mcgonigle, A.; Oppenheimer, C.; Allen, A.G. Characterization and evolution of tropospheric plumes from Lascar and Villarrica volcanoes, Chile. *J. Geophys. Res.* **2004**, *109*, D21303. [CrossRef]
13. Ridley, D.A.; Solomon, S.; Barnes, J.E.; Burlakov, V.D.; Deshler, T.; Dolgii, S.I.; Herber, A.B.; Nagai, T.; Neely, R.; Nevzorov, A.; et al. Total volcanic stratospheric aerosol optical depths and implications for global climate change. *Geophys. Res. Lett.* **2014**, *41*, 7763–7769. [CrossRef]

14. Vernier, J.-P.; Thomason, L.; Pommereau, J.-P.; Bourassa, A.; Pelon, J.; Garnier, A.; Hauchecorne, A.; Blanot, L.; Trepte, C.; Degenstein, D.; et al. Major influence of tropical volcanic eruptions on the stratospheric aerosol layer during the last decade. *Geophys. Res. Lett.* **2011**, *38*. [CrossRef]
15. Spinetti, C.; Buongiorno, M. Volcanic aerosol optical characteristics of Mt. Etna tropospheric plume retrieved by means of airborne multispectral images. *J. Atmos. Sol. Terr. Phys.* **2007**, *69*, 981–994. [CrossRef]
16. Sellitto, P.; Salerno, G.; La Spina, A.; Caltabiano, T.; Terray, L.; Gauthier, P.-J.; Briole, P. A novel methodology to determine volcanic aerosols optical properties in the UV and NIR and Ångström parameters using Sun photometry. *J. Geophys. Res. Atmos.* **2017**, *122*, 9803–9815. [CrossRef]
17. Porter, J.N.; Horton, K.A.; Mouginis-Mark, P.J.; Lienert, B.; Sharma, S.K.; Lau, E.; Sutton, A.J.; Elias, T.; Oppenheimer, C. Sun photometer and lidar measurements of the plume from the Hawaii Kilauea Volcano Pu'u O'o vent: Aerosol flux and SO_2 lifetime. *Geophys. Res. Lett.* **2002**, *29*, 30–31. [CrossRef]
18. Sellitto, P.; di Sarra, A.; Corradini, S.; Boichu, M.; Herbin, H.; Dubuisson, P.; Sèze, G.; Meloni, D.; Monteleone, F.; Merucci, L.; et al. Synergistic use of Lagrangian dispersion and radiative transfer modelling with satellite and surface remote sensing measurements for the investigation of volcanic plumes: The Mount Etna eruption of 25–27 October. *Atmos. Chem. Phys. Discuss.* **2016**, *16*, 6841–6861. [CrossRef]
19. Corradini, S.; Guerrieri, L.; Stelitano, D.; Salerno, G.; Scollo, S.; Merucci, L.; Prestifilippo, M.; Musacchio, M.; Silvestri, M.; Lombardo, V.; et al. Near real-time monitoring of the Christmas 2018 Etna eruption using SEVIRI and products validation. *Remote. Sens.* **2020**, *12*, 1336. [CrossRef]
20. Kloss, C.; Berthet, G.; Sellitto, P.; Ploeger, F.; Taha, G.; Tidiga, M.; Eremenko, M.; Bossolasco, A.; Jégou, F.; Renard, J.-B.; et al. Stratospheric aerosol layer perturbation caused by the 2019 Raikoke and Ulawun eruptions and their radiative forcing. *Atmos. Chem. Phys. Discuss.* **2021**, *21*, 535–560. [CrossRef]
21. Andersson, S.M.; Martinsson, B.G.; Vernier, J.-P.; Friberg, J.; Brenninkmeijer, C.A.M.; Hermann, M.; Van Velthoven, P.F.J.; Zahn, A. Significant radiative impact of volcanic aerosol in the lowermost stratosphere. *Nat. Commun.* **2015**, *6*, 7692. [CrossRef]
22. Guieu, C.; D'Ortenzio, F.; Dulac, F.; Taillandier, V.; Doglioli, A.; Petrenko, A.; Barrillon, S.; Mallet, M.; Nabat, P.; Desboeufs, K. Process studies at the air-sea interface after atmospheric deposition in the Mediterranean Sea: Objectives and strategy of the PEACETIME oceanographic campaign (May–June 2017). *Biogeosciences* **2020**, *17*, 5563–5585. [CrossRef]
23. Shcherbakov, V.; Jourdan, O.; Voigt, C.; Gayet, J.-F.; Chauvigne, A.; Schwarzenboeck, A.; Minikin, A.; Klingebiel, M.; Weigel, R.; Borrmann, S.; et al. Porous aerosol in degassing plumes of Mt. Etna and Mt. Stromboli. *Atmos. Chem. Phys. Discuss.* **2016**, *16*, 11883–11897. [CrossRef]
24. Sahyoun, M.; Freney, E.; Brito, J.; Duplissy, J.; Gouhier, M.; Colomb, A.; Dupuy, R.; Bourianne, T.; Nowak, J.B.; Yan, C.; et al. Evidence of new particle formation within Etna and Stromboli Volcanic plumes and its parameterization from airborne in situ measurements. *J. Geophys. Res. Atmos.* **2019**, *124*, 5650–5668. [CrossRef]
25. Pianezze, J.; Tulet, P.; Foucart, B.; Leriche, M.; Liuzzo, M.; Salerno, G.; Colomb, A.; Freney, E.; Sellegri, K. Volcanic plume aging during passive degassing and low eruptive events of Etna and Stromboli volcanoes. *J. Geophys. Res. Atmos.* **2019**, *124*, 11389–11405. [CrossRef]
26. Rosi, M.; Bertagnini, A.; Landi, P. Onset of the persistent activity at Stromboli Volcano (Italy). *Bull. Volcanol.* **2000**, *62*, 294–300. [CrossRef]
27. Barberi, F.; Rosi, M.; Sodi, A. Volcanic hazard assessment at Stromboli based on review of historical data. *Acta Vulcanol.* **1993**, *3*, 173–187.
28. Patrick, M.R.; Harris, A.J.L.; Ripepe, M.; Dehn, J.; Rothery, D.A.; Calvari, S. Strombolian explosive styles and source conditions: Insights from thermal (FLIR) video. *Bull. Volcanol.* **2007**, *69*, 769–784. [CrossRef]
29. Métrich, N.; Bertagnini, A.; Di Muro, A. Conditions of magma storage, degassing and ascent at Stromboli: New insights into the volcano plumbing system with inferences on the eruptive dynamics. *J. Petrol.* **2010**, *51*, 603–626. [CrossRef]
30. Bertagnini, A.; Métrich, N.; Landi, P.; Rosi, M. Stromboli volcano (Aeolian Archipelago, Italy): An open window on the deep-feeding system of a steady state basaltic volcano. *J. Geophys. Res.* **2003**, *108*, 2336. [CrossRef]
31. Calvari, S.; Spampinato, L.; Bonaccorso, A.; Oppenheimer, C.; Rivalta, E.; Boschi, E. Lava effusion—A slow fuse for paroxysms at Stromboli volcano? *Earth Planet. Sci. Lett.* **2011**, *301*, 317–323. [CrossRef]
32. Barberi, F.; Civetta, L.; Rosi, M.; Scandone, R. Chronology of the 2007 eruption of Stromboli and the activity of the Scientific Synthesis Group. *J. Volcanol. Geotherm. Res.* **2009**, *182*, 123–130. [CrossRef]
33. Allard, P.; Aiuppa, A.; Loyer, H.; Carrot, F.; Gaudry, A.; Pinte, G.; Michel, A.; Dongarrà, G. Acid gas and metal emission rates during long-lived basalt degassing at Stromboli Volcano. *Geophys. Res. Lett.* **2000**, *27*, 1207–1210. [CrossRef]
34. Allard, P.; Carbonnelle, J.; Métrich, N.; Loyer, H.; Zettwoog, P. Sulphur output and magma degassing budget of Stromboli volcano. *Nat. Cell Biol.* **1994**, *368*, 326–330. [CrossRef]
35. Allard, P.; Aiuppa, A.; Burton, M.; Caltabiano, T.; Federico, C.; Salerno, G.; La Spina, A. Crater gas emissions and the magma feeding system of Stromboli volcano. In *The Stromboli Volcano: An Integrated Study of the 2002–2003 Eruption*; Calvari, S., Inguaggiato, S., Puglisi, G., Ripepe, M., Rosi, M., Eds.; American Geophysical Union: Washington, DC, USA, 2008; Volume 182, pp. 65–80.

36. Aiuppa, A.; Inguaggiato, S.; Mcgonigle, A.; O'Dwyer, M.; Oppenheimer, C.; Padgett, M.; Rouwet, D.; Valenza, M. H2S fluxes from Mt. Etna, Stromboli, and Vulcano (Italy) and implications for the sulfur budget at volcanoes. *Geochim. Cosmochim. Acta* **2005**, *69*, 1861–1871. [CrossRef]
37. Aiuppa, A.; Bertagnini, A.; Métrich, N.; Moretti, R.; Di Muro, A.; Liuzzo, M.; Tamburello, G. A model of degassing for Stromboli volcano. *Earth Planet. Sci. Lett.* **2010**, *295*, 195–204. [CrossRef]
38. Global Volcanism Program. *Report on Stromboli (Italy)*; Crafford, A.E., Venzke, E., Eds.; Bulletin of the Global Volcanism Network, Smithsonian Institution: Washington, DC, USA, 2018. [CrossRef]
39. Stull, R.B. Mean boundary layer characteristics. In *An Introduction to Boundary Layer Meteorology*; Springer: Dordrecht, The Netherlands, 1988; pp. 1–27.
40. Morys, M.; Mims, F.M.; Hagerup, S.; Anderson, S.E.; Baker, A.; Kia, J.; Walkup, T. Design, calibration, and performance of MICROTOPS II handheld ozone monitor and Sun photometer. *J. Geophys. Res. Atmos.* **2001**, *106*, 14573–14582. [CrossRef]
41. Porter, J.N.; Miller, M.; Pietras, C.; Motell, C. Ship-based sun photometer measurements using microtops sun photometers. *J. Atmos. Ocean. Technol.* **2001**, *18*, 765–774. [CrossRef]
42. Watson, I.; Oppenheimer, C. Photometric observations of Mt. Etna's different aerosol plumes. *Atmos. Environ.* **2001**, *35*, 3561–3572. [CrossRef]
43. Kloss, C.; Berthet, G.; Sellitto, P.; Ploeger, F.; Bucci, S.; Khaykin, S.; Jégou, F.; Taha, G.; Thomason, L.W.; Barret, B.; et al. Transport of the 2017 Canadian wildfire plume to the tropics via the Asian monsoon circulation. *Atmos. Chem. Phys. Discuss.* **2019**, *19*, 13547–13567. [CrossRef]
44. Schulz, M.; Textor, C.; Kinne, S.; Balkanski, Y.; Bauer, S.; Berntsen, T.; Berglen, T.; Boucher, O.; Dentener, F.; Guibert, S.; et al. Radiative forcing by aerosols as derived from the AeroCom present-day and pre-industrial simulations. *Atmos. Chem. Phys. Discuss.* **2006**, *6*, 5225–5246. [CrossRef]
45. Reed, B.E.; Peters, D.M.; McPheat, R.; Grainger, R.G. The Complex refractive index of volcanic ash aerosol retrieved from spectral mass extinction. *J. Geophys. Res. Atmos.* **2018**, *123*, 1339–1350. [CrossRef]
46. Watson, I.M.; Oppenheimer, C. Particle size distributions of Mount Etna's aerosol plume constrained by Sun photometry. *J. Geophys. Res.* **2000**, *105*, 9823–9829. [CrossRef]